

# Light-Cone Wavefunction Representations of Sivers and Boer-Mulders Distribution Functions

Dae Sung Hwang

*Department of Physics, Sejong University, Seoul 143-747, South Korea*

## Abstract

We find the light-cone wavefunction representations of the Sivers and Boer-Mulders distribution functions. A necessary condition for the existence of these representations is that the light-cone wavefunctions have complex phases. We induce the complex phases by incorporating the final-state interactions into the light-cone wavefunctions. For the scalar and axial-vector diquark models for nucleon, we calculate explicitly the Sivers and Boer-Mulders distribution functions from the light-cone wavefunction representations. We obtain the results that the Sivers distribution function has the opposite signs with the factor 3 difference in magnitude for the two models, whereas the Boer-Mulders distribution function has the same sign and magnitude. We can understand these results from the properties of the light-cone wavefunction representations of the Sivers and Boer-Mulders distribution functions.

PACS codes: 13.40.Gp, 13.60.-r, 13.88.+e, 14.20.Dh

Key words: Spin, Light-cone Wavefunction, Sivers Function, Boer-Mulders Function

# 1 Introduction

It was found that the final-state interaction of quark and gluon induces the single-spin asymmetry in the semi-inclusive deep inelastic scattering at the twist-two level [1]. Then, this time-odd twist-two effect was interpreted as the Sivers effect [2] by finding that the final-state interaction can be treated as the source of the time-odd Sivers distribution function [3, 4, 5, 6, 7]. It is also often referred to as “naively  $T$ -odd”, because the appearance of this function does not imply a violation of time-reversal invariance, since they can arise through the final-state interactions. With these developments, the existence of the Sivers distribution function has gained a firm theoretical support. The Sivers distribution function  $f_{1T}^\perp$  describes the difference between the momentum distributions of unpolarized quark inside the nucleons transversely polarized in opposite directions. There is another quark distribution function of the nucleon induced by the final-state interaction of quark and gluon, which is called the Boer-Mulders distribution function  $h_1^\perp$  [8].  $h_1^\perp$  describes the difference between the momentum distributions of the quarks transversely polarized in opposite directions inside unpolarized nucleon. The distribution functions  $f_{1T}^\perp$  and  $h_1^\perp$  are depicted in Figs. 1 and 2.

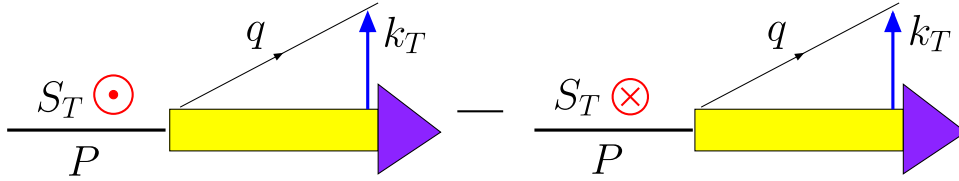


Figure 1: *Schematic depiction of the Sivers distribution function  $f_{1T}^\perp$ . The spin vector  $S_T$  of the nucleon points out of and into the page, respectively, and  $k_T$  is the transverse momentum of the extracted quark.*

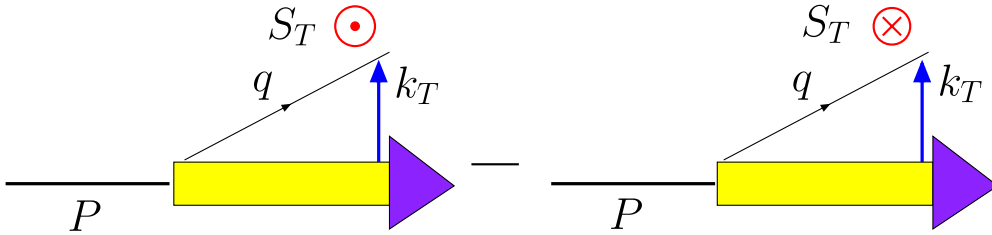


Figure 2: *Schematic depiction of the Boer-Mulders distribution function  $h_1^\perp$ . The spin vector  $S_T$  of the quark points out of and into the page, respectively, and  $k_T$  is the transverse momentum of the extracted quark.*

The light-cone wavefunctions are valuable for studying the hadronic processes by treating the non-perturbative effects in a relativistically covariant way [9, 10]. The formulas which express the electromagnetic form factors and the generalized parton distribution functions in terms of the light-cone wavefunctions were found in Refs. [11, 12, 13] and Refs. [14, 15], respectively. In Ref. [16] the light-cone wavefunction representation of the nucleon electric dipole moment was found by introducing the complex phases of the light-cone wavefunctions, and studied a general relation connecting nucleon electric dipole and anomalous magnetic moments.

In this paper we derive the formulas which express the Sivers and Boer-Mulders distribution functions in terms of the matrix elements of the nucleon spin states. Then we derive the light-cone

wavefunction representations of the Siverson and Boer-Mulders distribution functions, and we calculate these functions for the scalar and axial-vector diquark models by using these representations.

The light-cone wavefunction representations show that the Siverson distribution function is given by the overlap of the wavefunctions of the same quark spin states of the opposite nucleon spin states, whereas the Boer-Mulders distribution function is given by the overlap of the wavefunctions of the opposite quark spin states within a given nucleon spin state. From these properties of their light-cone wavefunction representations, we can understand why the Siverson distribution function has the opposite signs with the factor 3 difference in magnitude for the scalar and axial-vector diquark models, whereas the Boer-Mulders distribution function has the same sign and magnitude for these diquark models.

## 2 Siverson and Boer-Mulders Distribution Functions

The  $k_T$ -dependent unpolarized quark distribution function  $f_1(x, \vec{k}_\perp)$ , the Siverson distribution function  $f_{1T}^\perp(x, \vec{k}_\perp)$  and the Boer-Mulders distribution function  $h_1^\perp(x, \vec{k}_\perp)$  are parts of the proton correlation function  $\Phi(x, \vec{k}_\perp : P, S)$  [8]:

$$\Phi(x, \vec{k}_\perp : P, S) = \frac{M}{2P^+} \left[ f_1(x, \vec{k}_\perp) \frac{\gamma \cdot P}{M} + f_{1T}^\perp(x, \vec{k}_\perp) \epsilon_{\mu\nu\rho\sigma} \frac{\gamma^\mu P^\nu k_\perp^\rho S_T^\sigma}{M^2} + h_1^\perp(x, \vec{k}_\perp) \frac{\sigma_{\mu\nu} k_\perp^\mu P^\nu}{M^2} + \dots \right], \quad (1)$$

from which we find that  $f_1(x, \vec{k}_\perp)$  and  $f_{1T}^\perp(x, \vec{k}_\perp)$  can be defined through matrix elements of the bilinear vector current:

$$\begin{aligned} & \int \frac{dy^- d^2 \vec{y}_\perp}{16\pi^3} e^{ixP^+ y^- - i\vec{k}_\perp \cdot \vec{y}_\perp} \langle P, \vec{S}_\perp | \bar{\psi}(0) \gamma^+ \psi(y) | P, \vec{S}_\perp \rangle \Big|_{y^+=0} \\ &= \frac{1}{2P^+} \left[ f_1(x, \vec{k}_\perp) \bar{U}(P, \vec{S}_\perp) \gamma^+ U(P, \vec{S}_\perp) + f_{1T}^\perp(x, \vec{k}_\perp) \frac{k_\perp^i}{M} \bar{U}(P, \vec{S}_\perp) \sigma^{i+} U(P, \vec{S}_\perp) \right], \end{aligned} \quad (2)$$

where

$$\frac{1}{2P^+} \bar{U}(P, \vec{S}_\perp) \sigma^{i+} U(P, \vec{S}_\perp) = \epsilon^{ji} S_\perp^j \quad \text{with } \epsilon^{12} = -\epsilon^{21} = 1. \quad (3)$$

For an explicit calculation, let us consider the case of  $\vec{S}_\perp = (S_\perp^1, S_\perp^2) = (0, 1)$  for the transverse spin in (2). Then, the proton state is given by  $(|P, \uparrow\rangle + i|P, \downarrow\rangle)/\sqrt{2}$  and Eq. (2) becomes

$$\mathcal{B} \frac{\langle P, \uparrow | -i \langle P, \downarrow | \bar{\psi}(0) \gamma^+ \psi(y) | P, \uparrow \rangle + i | P, \downarrow \rangle}{\sqrt{2}} \Big|_{y^+=0} = f_1(x, \vec{k}_\perp) - S_\perp^2 \frac{k_\perp^1}{M} f_{1T}^\perp(x, \vec{k}_\perp), \quad (4)$$

where

$$\mathcal{B} \equiv \int \frac{dy^- d^2 \vec{y}_\perp}{16\pi^3} e^{ixP^+ y^- - i\vec{k}_\perp \cdot \vec{y}_\perp}. \quad (5)$$

From (4) we have

$$f_1(x, \vec{k}_\perp) = \mathcal{B} \frac{1}{2} \left[ \langle P, \uparrow | J^+(y) | P, \uparrow \rangle + \langle P, \downarrow | J^+(y) | P, \downarrow \rangle \right] \Big|_{y^+=0}, \quad (6)$$

$$-\frac{k_\perp^1}{M} f_{1T}^\perp(x, \vec{k}_\perp) = \mathcal{B} \frac{i}{2} \left[ \langle P, \uparrow | J^+(y) | P, \downarrow \rangle - \langle P, \downarrow | J^+(y) | P, \uparrow \rangle \right] \Big|_{y^+=0}, \quad (7)$$

where  $J^+(y) = \bar{\psi}(0) \gamma^+ \psi(y)$ .

On the other hand, from (1) the Boer-Mulders distribution function  $h_1^\perp(x, \vec{k}_\perp)$  can be defined through matrix elements of the bilinear tensor current:

$$\begin{aligned} & \int \frac{dy^- d^2\vec{y}_\perp}{16\pi^3} e^{ixP^+y^- - i\vec{k}_\perp \cdot \vec{y}_\perp} \langle P, \vec{S}_\perp | \bar{\psi}(0) \sigma^{i+} \psi(y) | P, \vec{S}_\perp \rangle \Big|_{y^+=0} \\ &= \frac{1}{2P^+} \left[ h_1^\perp(x, \vec{k}_\perp) \frac{k_\perp^i}{M} \bar{U}(P, \vec{S}_\perp) \gamma^+ U(P, \vec{S}_\perp) \right], \end{aligned} \quad (8)$$

which gives

$$\frac{k_\perp^i}{M} h_1^\perp(x, \vec{k}_\perp) = \frac{1}{2} \mathcal{B} \left( \left[ \langle P, \uparrow | \bar{\psi}(0) \sigma^{i+} \psi(y) | P, \uparrow \rangle \right] + \left[ \langle P, \downarrow | \bar{\psi}(0) \sigma^{i+} \psi(y) | P, \downarrow \rangle \right] \right) \Big|_{y^+=0}. \quad (9)$$

### 3 Light-Cone Wavefunction Representations of Sivers and Boer-Mulders Functions

The expansion of the proton eigensolution  $|\psi_p\rangle$  on the eigenstates  $\{|n\rangle\}$  of the free Hamiltonian  $H_{LC}$  gives the light-cone Fock expansion:

$$\begin{aligned} |\psi_p(P^+, \vec{P}_\perp)\rangle &= \sum_n \prod_{i=1}^n \frac{dx_i d^2\vec{k}_{\perp i}}{\sqrt{x_i} 16\pi^3} 16\pi^3 \delta\left(1 - \sum_{i=1}^n x_i\right) \delta^{(2)}\left(\sum_{i=1}^n \vec{k}_{\perp i}\right) \\ &\quad \times \psi_n(x_i, \vec{k}_{\perp i}, \lambda_i) |n; x_i P^+, x_i \vec{P}_\perp + \vec{k}_{\perp i}, \lambda_i\rangle. \end{aligned} \quad (10)$$

The plus component momentum fractions  $x_i = k_i^+/P^+$  and the transverse momenta  $\vec{k}_{\perp i}$  of partons represent the relative momentum coordinates of the light-cone wavefunctions. The physical transverse momenta of partons are  $\vec{p}_{\perp i} = x_i \vec{P}_\perp + \vec{k}_{\perp i}$ . The  $\lambda_i$  label the light-cone spin projections of the partons along the quantization direction  $z$ . The  $n$ -particle states are normalized as

$$\langle n; p_i'^+, \vec{p}'_{\perp i}, \lambda'_i | n; p_i^+, \vec{p}_{\perp i}, \lambda_i \rangle = \prod_{i=1}^n 16\pi^3 p_i^+ \delta(p_i'^+ - p_i^+) \delta^{(2)}(\vec{p}'_{\perp i} - \vec{p}_{\perp i}) \delta_{\lambda'_i \lambda_i}. \quad (11)$$

From (6) and (7) we get

$$f_1(x, \vec{k}_\perp) = \mathcal{C} \frac{1}{2} \left[ \psi_{(n)}^{\uparrow*}(x_i, \vec{k}_{\perp i}, \lambda_i) \psi_{(n)}^\uparrow(x_i, \vec{k}_{\perp i}, \lambda_i) + \psi_{(n)}^{\downarrow*}(x_i, \vec{k}_{\perp i}, \lambda_i) \psi_{(n)}^\downarrow(x_i, \vec{k}_{\perp i}, \lambda_i) \right], \quad (12)$$

$$-\frac{k_\perp^1}{M} f_{1T}^\perp(x, \vec{k}_\perp) = \mathcal{C} \frac{i}{2} \left[ \psi_{(n)}^{\uparrow*}(x_i, \vec{k}_{\perp i}, \lambda_i) \psi_{(n)}^\downarrow(x_i, \vec{k}_{\perp i}, \lambda_i) - \psi_{(n)}^{\downarrow*}(x_i, \vec{k}_{\perp i}, \lambda_i) \psi_{(n)}^\uparrow(x_i, \vec{k}_{\perp i}, \lambda_i) \right], \quad (13)$$

where

$$\mathcal{C} \equiv \sum_{n, \lambda_i} \int \prod_{i=1}^n \frac{dx_i d^2\vec{k}_{\perp i}}{16\pi^3} 16\pi^3 \delta\left(1 - \sum_{j=1}^n x_j\right) \delta^{(2)}\left(\sum_{j=1}^n \vec{k}_{\perp j}\right) \delta(x - x_1) \delta^{(2)}(\vec{k}_\perp - \vec{k}_{\perp 1}). \quad (14)$$

As we see in (13), the Sivers distribution function is given by the product of the light-cone wavefunctions which have opposite proton spin states and same quark spin states.

From (9) we have

$$\begin{aligned}
\frac{k_{\perp}^1}{M} h_1^{\perp}(x, \vec{k}_{\perp}) &= \frac{\mathcal{C}}{2} (-i) \left( \left[ \psi_{(n)}^{\uparrow*}(x_i, \vec{k}_{\perp i}, \lambda'_1 = \downarrow, \lambda_{i \neq 1}) \psi_{(n)}^{\uparrow}(x_i, \vec{k}_{\perp i}, \lambda_1 = \uparrow, \lambda_{i \neq 1}) \right. \right. \\
&\quad \left. \left. - \psi_{(n)}^{\uparrow*}(x_i, \vec{k}_{\perp i}, \lambda'_1 = \uparrow, \lambda_{i \neq 1}) \psi_{(n)}^{\uparrow}(x_i, \vec{k}_{\perp i}, \lambda_1 = \downarrow, \lambda_{i \neq 1}) \right] \right. \\
&\quad \left. + \left[ \psi_{(n)}^{\downarrow*}(x_i, \vec{k}_{\perp i}, \lambda'_1 = \downarrow, \lambda_{i \neq 1}) \psi_{(n)}^{\downarrow}(x_i, \vec{k}_{\perp i}, \lambda_1 = \uparrow, \lambda_{i \neq 1}) \right. \right. \\
&\quad \left. \left. - \psi_{(n)}^{\downarrow*}(x_i, \vec{k}_{\perp i}, \lambda'_1 = \uparrow, \lambda_{i \neq 1}) \psi_{(n)}^{\downarrow}(x_i, \vec{k}_{\perp i}, \lambda_1 = \downarrow, \lambda_{i \neq 1}) \right] \right). \quad (15)
\end{aligned}$$

As we see in (15), the Boer-Mulders distribution function is given by the product of the light-cone wavefunctions which have same proton spin states and opposite quark spin states, whereas we found in (13) that the Sivers distribution function is given by the product of the light-cone wavefunctions which have opposite proton spin states and same quark spin states.

## 4 Explicit Calculations in Diquark Models

### 4.1 Scalar Diquark Model

In this subsection we calculate the Sivers and Boer-Mulders distribution functions of the scalar diquark model by using the light-cone wavefunction representations derived in section 3. In the scalar diquark model, the  $J^z = +\frac{1}{2}$  two particle Fock state is given by [1, 13]

$$\begin{aligned}
& \left| \Psi_{\text{two particle}}^{\uparrow}(P^+ = 1, \vec{P}_{\perp} = \vec{0}_{\perp}) \right\rangle \quad (16) \\
&= \int \frac{dx d^2 \vec{k}_{\perp}}{\sqrt{x(1-x)} 16\pi^3} \left[ \psi_{+\frac{1}{2}}^{\uparrow}(x, \vec{k}_{\perp}) \left| +\frac{1}{2}; x, \vec{k}_{\perp} \right\rangle + \psi_{-\frac{1}{2}}^{\uparrow}(x, \vec{k}_{\perp}) \left| -\frac{1}{2}; x, \vec{k}_{\perp} \right\rangle \right],
\end{aligned}$$

where

$$\begin{cases} \psi_{+\frac{1}{2}}^{\uparrow}(x, \vec{k}_{\perp}) = \frac{(m+xM)}{x} \varphi, \\ \psi_{-\frac{1}{2}}^{\uparrow}(x, \vec{k}_{\perp}) = -\frac{(+k^1 + ik^2)}{x} \varphi. \end{cases} \quad (17)$$

The scalar part of the wavefunction  $\varphi$  is given by

$$\varphi(x, \vec{k}_{\perp}) = \frac{g}{\sqrt{1-x}} \frac{1}{M^2 - \frac{\vec{k}_{\perp}^2 + m^2}{x} - \frac{\vec{k}_{\perp}^2 + \lambda^2}{1-x}} = -g \frac{x\sqrt{1-x}}{\vec{k}_{\perp}^2 + B}, \quad (18)$$

where

$$B = x(1-x) \left( -M^2 + \frac{m^2}{x} + \frac{\lambda^2}{1-x} \right). \quad (19)$$

Similarly, the  $J^z = -\frac{1}{2}$  two particle Fock state is given by

$$\begin{aligned}
& \left| \Psi_{\text{two particle}}^{\downarrow}(P^+ = 1, \vec{P}_{\perp} = \vec{0}_{\perp}) \right\rangle \quad (20) \\
&= \int \frac{dx d^2 \vec{k}_{\perp}}{\sqrt{x(1-x)} 16\pi^3} \left[ \psi_{+\frac{1}{2}}^{\downarrow}(x, \vec{k}_{\perp}) \left| +\frac{1}{2}; x, \vec{k}_{\perp} \right\rangle + \psi_{-\frac{1}{2}}^{\downarrow}(x, \vec{k}_{\perp}) \left| -\frac{1}{2}; x, \vec{k}_{\perp} \right\rangle \right],
\end{aligned}$$

where

$$\begin{cases} \psi_{+\frac{1}{2}}^\downarrow(x, \vec{k}_\perp) = -\frac{(-k^1 + ik^2)}{x} \varphi, \\ \psi_{-\frac{1}{2}}^\downarrow(x, \vec{k}_\perp) = \frac{(m+xM)}{x} \varphi. \end{cases} \quad (21)$$

The coefficients of  $\varphi$  in Eqs. (17) and (21) are the matrix elements of  $\frac{\bar{u}(k^+, k^-, \vec{k}_\perp) u(P^+, P^-, \vec{P}_\perp)}{\sqrt{k^+} \sqrt{P^+}}$  which are the numerators of the wavefunctions corresponding to each constituent spin  $s^z$  configuration.

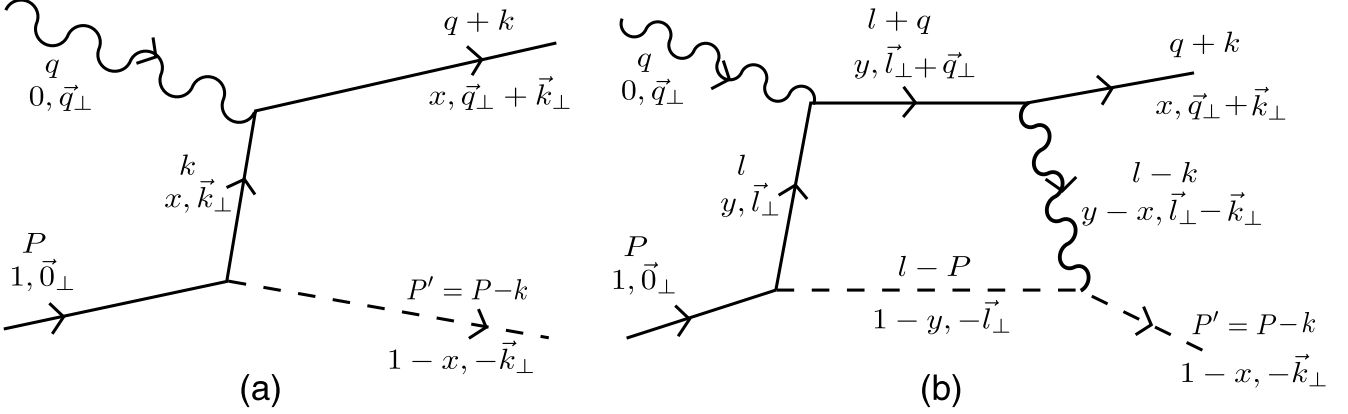


Figure 3: (a) Tree level diagram and (b) diagram with final-state interaction.

In Ref. [1] it was found that the contributing amplitudes for  $\gamma^* p \rightarrow q(qq)_0$  are given by the following formulas through one loop order which is depicted in Fig. 3:

$$\mathcal{A}(\uparrow \rightarrow \uparrow) = \frac{(m+xM)}{x} C \left( h + i \frac{e_1 e_2}{8\pi} g_1 \right) \quad (22)$$

$$\mathcal{A}(\uparrow \rightarrow \downarrow) = -\frac{(+k^1 + ik^2)}{x} C \left( h + i \frac{e_1 e_2}{8\pi} g_2 \right) \quad (23)$$

$$\mathcal{A}(\downarrow \rightarrow \uparrow) = -\frac{(-k^1 + ik^2)}{x} C \left( h + i \frac{e_1 e_2}{8\pi} g_2 \right) \quad (24)$$

$$\mathcal{A}(\downarrow \rightarrow \downarrow) = \frac{(m+xM)}{x} C \left( h + i \frac{e_1 e_2}{8\pi} g_1 \right), \quad (25)$$

where

$$C = -g e_1 P^+ \sqrt{x} 2x(1-x) \quad (26)$$

$$h = \frac{1}{\vec{k}_\perp^2 + x(1-x)(-M^2 + \frac{m^2}{x} + \frac{\lambda^2}{1-x})}, \quad (27)$$

and

$$g_1 = \int_0^1 d\alpha \frac{-1}{\alpha(1-\alpha)\vec{k}_\perp^2 + \alpha\lambda_g^2 + (1-\alpha)B}, \quad (28)$$

$$g_2 = \int_0^1 d\alpha \frac{-\alpha}{\alpha(1-\alpha)\vec{k}_\perp^2 + \alpha\lambda_g^2 + (1-\alpha)B}. \quad (29)$$

In the above,  $e_1$  and  $e_2$  are the quark and diquark charge, and  $M$ ,  $m$ ,  $\lambda$  and  $\lambda_g$  are the nucleon, quark, diquark and gluon mass, respectively. Ref. [1] fixed  $\frac{e_1 e_2}{4\pi} = -C_F \alpha_S$ , where  $C_F = \frac{4}{3}$  in order to relate the above results to QCD. We take  $\lambda_g = 0$  at the end of the calculation. We note that the results (28) and (29) are for the semi-inclusive deep inelastic scattering, and the results for the Drell-Yan process have opposite signs compared to (28) and (29) [3, 17].

The final-state interactions in semi-inclusive deep inelastic scattering are commonly treated as a part of the proton distribution function [3, 6]. If we adopt the same treatment for the wavefunctions, we can consider that the final-state interactions for the scalar diquark model depicted in Fig. 3 induce the spin-dependent complex phases to the wavefunctions [18]:

$$\begin{cases} \psi_{+\frac{1}{2}}^\uparrow(x, \vec{k}_\perp) = \frac{(m+xM)}{x} (1 + ia_1) \varphi, \\ \psi_{-\frac{1}{2}}^\uparrow(x, \vec{k}_\perp) = -\frac{(+k^1 + ik^2)}{x} (1 + ia_2) \varphi, \end{cases} \quad (30)$$

$$\begin{cases} \psi_{+\frac{1}{2}}^\downarrow(x, \vec{k}_\perp) = -\frac{(-k^1 + ik^2)}{x} (1 + ia_2) \varphi, \\ \psi_{-\frac{1}{2}}^\downarrow(x, \vec{k}_\perp) = \frac{(m+xM)}{x} (1 + ia_1) \varphi, \end{cases} \quad (31)$$

where  $a_1$  and  $a_2$  are given by

$$a_{1,2} = \frac{e_1 e_2}{8\pi} (\vec{k}_\perp^2 + B) g_{1,2} \quad (32)$$

with  $g_{1,2}$  given in (28) and (29).

Using the wavefunctions (30) and (31) in the formulas (12), (13) and (15), we obtain

$$f_1(x, \vec{k}_\perp) = \frac{1}{16\pi^3} \left[ (M + \frac{m}{x})^2 + \frac{\vec{k}_\perp^2}{x^2} \right] \varphi^2, \quad (33)$$

$$f_{1T}^\perp(x, \vec{k}_\perp) = \frac{1}{16\pi^3} 2 \frac{M}{x} (M + \frac{m}{x}) \varphi^2 \frac{e_1 e_2}{8\pi} (\vec{k}_\perp^2 + B) \frac{1}{\vec{k}_\perp^2} \ln \frac{(\vec{k}_\perp^2 + B)}{B}, \quad (34)$$

$$h_1^\perp(x, \vec{k}_\perp) = \frac{1}{16\pi^3} 2 \frac{M}{x} (M + \frac{m}{x}) \varphi^2 \frac{e_1 e_2}{8\pi} (\vec{k}_\perp^2 + B) \frac{1}{\vec{k}_\perp^2} \ln \frac{(\vec{k}_\perp^2 + B)}{B}. \quad (35)$$

The results in (34) and (35) agree with those in Refs. [1, 6] with an additional overall minus sign which should be corrected [19].

## 4.2 Axial-Vector Diquark Model

Jakob et al. [20] studied the scalar ( $s$ ) and axial-vector ( $a$ ) diquark models using the following nucleon-quark-diquark vertices:

$$\Upsilon_s = g_s(k^2), \quad \Upsilon_a^\mu = \frac{g_a(k^2)}{\sqrt{3}} \gamma^\mu \gamma_5, \quad (36)$$

where  $g_s(k^2)$  and  $g_a(k^2)$  are form factors which we take as 1 in this paper for simplicity. We can then obtain the light-cone wavefunctions of scalar and axial-vector diquark models from Fig. 4. In Ref. [20],  $\gamma_5(\gamma^\mu + \frac{P^\mu}{M})$  appears at the vertex of the axial-vector diquark model instead of just  $\gamma^\mu \gamma_5$  appearing in (36). However, (36) is equivalent to the vertex of Ref. [20] since  $\frac{P^\mu}{M}$  vanishes when the polarization sum  $\sum_\lambda \epsilon_\mu^{*(\lambda)} \epsilon_\nu^{(\lambda)} = -g_{\mu\nu} + P_\mu P_\nu / M^2$ , which Ref. [20] used, is multiplied.

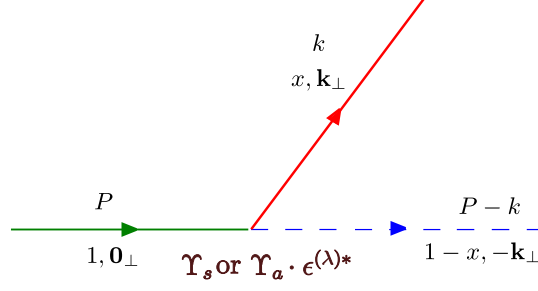


Figure 4: Diagram giving the light-cone wavefunctions of scalar and axial-vector diquark models.

In order to obtain the light-cone wavefunctions of axial-vector diquark model, we decompose the polarization sum  $\sum_\lambda \epsilon_\mu^{*(\lambda)} \epsilon_\nu^{(\lambda)} = -g_{\mu\nu} + P_\mu P_\nu / M^2$  of Ref. [20] to the following three polarization vectors  $\epsilon^{\mu(\lambda)}$ :

$$\begin{aligned}
\epsilon^{\mu(+1)} &= (\epsilon^{0(+1)}, \epsilon^{1(+1)}, \epsilon^{2(+1)}, \epsilon^{3(+1)}) = \frac{1}{\sqrt{2}}(0, -1, -i, 0), \\
\epsilon^{\mu(-1)} &= \frac{1}{\sqrt{2}}(0, +1, -i, 0), \\
\epsilon^{\mu(0)} &= \left(\frac{P^3}{M}, 0, 0, \frac{P^0}{M}\right).
\end{aligned} \tag{37}$$

In order to calculate the effects of the final-state interactions, we use for the gauge-field coupling to the axial-vector diquark in Fig. 3 the simple form  $ie_2 g^{\alpha\beta} ((P-l) + (P-k))^\mu$ , which is equivalent, for each polarization state, to the gauge-field coupling to a scalar diquark [21]. We motivate this simple coupling by assuming that the QCD coupling to the diquark is independent of the spin state of the diquark.

The two-particle Fock state for proton with  $J^z = +\frac{1}{2}$  (positive helicity) has six possible spin combinations for the quark and axial-vector diquark:

$$\begin{aligned}
\left| \Psi_{\text{two particle}}^\uparrow(P^+, \vec{P}_\perp = \vec{0}_\perp) \right\rangle &= \int \frac{dx d^2\vec{k}_\perp}{\sqrt{x(1-x)} 16\pi^3} \\
&\left[ \psi_{+\frac{1}{2}+1}^\uparrow(x, \vec{k}_\perp) \left| +\frac{1}{2} + 1; xP^+, \vec{k}_\perp \right\rangle + \psi_{+\frac{1}{2}-1}^\uparrow(x, \vec{k}_\perp) \left| -\frac{1}{2} + 1; xP^+, \vec{k}_\perp \right\rangle \right. \\
&+ \psi_{-\frac{1}{2}+1}^\uparrow(x, \vec{k}_\perp) \left| +\frac{1}{2} 0; xP^+, \vec{k}_\perp \right\rangle + \psi_{-\frac{1}{2}-1}^\uparrow(x, \vec{k}_\perp) \left| -\frac{1}{2} 0; xP^+, \vec{k}_\perp \right\rangle \\
&\left. + \psi_{-\frac{1}{2}+1}^\uparrow(x, \vec{k}_\perp) \left| +\frac{1}{2} - 1; xP^+, \vec{k}_\perp \right\rangle + \psi_{-\frac{1}{2}-1}^\uparrow(x, \vec{k}_\perp) \left| -\frac{1}{2} - 1; xP^+, \vec{k}_\perp \right\rangle \right],
\end{aligned} \tag{38}$$

where the two-particle states  $|s_f^z, s_b^z; x, \vec{k}_\perp\rangle$  are normalized as in (11).  $s_f^z$  and  $s_b^z$  denote the  $z$ -component of the spins of the constituent fermion and boson, respectively, and the variables  $x$



and  $\vec{k}_\perp$  refer to the momentum of the fermion. The wavefunctions are given by [21]

$$\left\{ \begin{array}{l} \psi_{+\frac{1}{2}+1}^\uparrow(x, \vec{k}_\perp) = -\sqrt{\frac{2}{3}} \frac{(-k^1+ik^2)}{x} (1+ia_2) \varphi, \\ \psi_{-\frac{1}{2}+1}^\uparrow(x, \vec{k}_\perp) = +\sqrt{\frac{2}{3}} \frac{(m+xM)}{x} (1+ia_1) \varphi, \\ \psi_{+\frac{1}{2}0}^\uparrow(x, \vec{k}_\perp) = -\sqrt{\frac{1}{3}} \frac{(m+xM)}{x} (1+ia_1) \varphi, \\ \psi_{-\frac{1}{2}0}^\uparrow(x, \vec{k}_\perp) = +\sqrt{\frac{1}{3}} \frac{(+k^1+ik^2)}{x} (1+ia_2) \varphi, \\ \psi_{+\frac{1}{2}-1}^\uparrow(x, \vec{k}_\perp) = 0, \\ \psi_{-\frac{1}{2}-1}^\uparrow(x, \vec{k}_\perp) = 0, \end{array} \right. \quad (39)$$

where the scalar part of the wavefunction  $\varphi(x, \vec{k}_\perp)$  is given in (18).

Similarly, the wavefunctions for proton with  $J^z = -\frac{1}{2}$  (negative helicity) are given by [21]

$$\left\{ \begin{array}{l} \psi_{+\frac{1}{2}+1}^\downarrow(x, \vec{k}_\perp) = 0, \\ \psi_{-\frac{1}{2}+1}^\downarrow(x, \vec{k}_\perp) = 0, \\ \psi_{+\frac{1}{2}0}^\downarrow(x, \vec{k}_\perp) = -\sqrt{\frac{1}{3}} \frac{(-k^1+ik^2)}{x} (1+ia_2) \varphi, \\ \psi_{-\frac{1}{2}0}^\downarrow(x, \vec{k}_\perp) = +\sqrt{\frac{1}{3}} \frac{(m+xM)}{x} (1+ia_1) \varphi, \\ \psi_{+\frac{1}{2}-1}^\downarrow(x, \vec{k}_\perp) = -\sqrt{\frac{2}{3}} \frac{(m+xM)}{x} (1+ia_1) \varphi, \\ \psi_{-\frac{1}{2}-1}^\downarrow(x, \vec{k}_\perp) = +\sqrt{\frac{2}{3}} \frac{(+k^1+ik^2)}{x} (1+ia_2) \varphi. \end{array} \right. \quad (40)$$

In Eqs. (39) and (40)  $a_1$  and  $a_2$  are given by (32), and the coefficients of  $\varphi$  are the matrix elements of  $\frac{\bar{u}(k^+, k^-, \vec{k}_\perp)}{\sqrt{k^+}} \gamma \cdot \epsilon^* \frac{u(P^+, P^-, \vec{P}_\perp)}{\sqrt{P^+}}$  which are the numerators of the wavefunctions corresponding to each constituent spin  $s^z$  configuration.

Using the wavefunctions given in (39) and (40) in the formulas (12) and (13), we obtain

$$f_1(x, \vec{k}_\perp) = \frac{1}{16\pi^3} \left[ (M + \frac{m}{x})^2 + \frac{\vec{k}_\perp^2}{x^2} \right] \varphi^2, \quad (41)$$

$$f_{1T}^\perp(x, \vec{k}_\perp) = -\frac{1}{3} \frac{1}{16\pi^3} 2 \frac{M}{x} (M + \frac{m}{x}) \varphi^2 \frac{e_1 e_2}{8\pi} (\vec{k}_\perp^2 + B) \frac{1}{\vec{k}_\perp^2} \ln \frac{(\vec{k}_\perp^2 + B)}{B}. \quad (42)$$

In the same way, by using the wavefunctions given in (39) and (40) in the formula (15), we obtain the Boer-Mulders distribution function as

$$h_1^\perp(x, \vec{k}_\perp) = \frac{1}{16\pi^3} 2 \frac{M}{x} (M + \frac{m}{x}) \varphi^2 \frac{e_1 e_2}{8\pi} (\vec{k}_\perp^2 + B) \frac{1}{\vec{k}_\perp^2} \ln \frac{(\vec{k}_\perp^2 + B)}{B}. \quad (43)$$

The Sivers distribution function  $f_{1T}^\perp$  is given by the overlaps of the proton wavefunctions of positive and negative helicities [1, 6]. As we can see in (39) and (40), only the wavefunctions with  $s_b^z = 0$  contribute to the overlaps for  $f_{1T}^\perp$ . We find that the wavefunctions with  $s_b^z = 0$  in (39) and (40) have the exactly same structures as the wavefunctions for the quark and scalar diquark system given in (30) and (31), except for the overall constant factor  $-\frac{1}{\sqrt{3}}$  for the positive helicity wavefunctions and  $+\frac{1}{\sqrt{3}}$  for the negative helicity ones. These constant factors can be understood

	Sivers Function	Boer-Mulders Function
Scalar Diquark Model	-1	-1
Axial-Vector Diquark Model	$+\frac{1}{3}$	-1

Table 1: Relative signs and magnitudes of Sivers and Boer-Mulders distribution functions in scalar and axial-vector diquark models.

by the Clebsch-Gordan coefficients for the combination of spin  $\frac{1}{2}$  and spin 1 states [21]. Therefore, the overlaps of positive and negative helicities for the quark and axial-vector diquark system have an overall factor of  $-\frac{1}{3}$  compared to the overlaps of (30) and (31) for the quark and scalar diquark system. This is the reason why, in the diquark models with which we work in this paper, we have the same Sivers distribution functions for the cases of the scalar diquark and axial-vector diquark, except for the difference of the additional overall constant factor  $-\frac{1}{3}$  of the axial-vector diquark model [21], as we can see in (34) and (42).

On the other hand, the Boer-Mulders distribution function  $h_1^\perp$  is given by the overlaps of the wavefunctions of opposite quark spin states within a given proton helicity state. Concerning the two quark spin states for a fixed  $s_b^z$  value within a given proton helicity state, the wavefunctions in (39) and (40) have the same structures as the wavefunctions of the scalar diquark model given in (30) and (31). This structure is given by the relation between the light-cone and Bjorken-Drell spinors [21]. Therefore, the Boer-Mulders distribution of the axial-vector diquark model is the same as that of the scalar diquark model as we can see in (35) and (43). We summarize the results in Table 1. We note that Ref. [22] studied the Boer-Mulders distribution functions  $h_1^\perp$  for a variety of phenomenological models and found that the signs of  $h_1^\perp$  are all negative for the models which they studied.

## 5 Conclusion

In this paper we find the light-cone wavefunction representations of the Sivers and Boer-Mulders distribution functions. A necessary condition for the existence of these representations is that the light-cone wavefunctions have complex phases. We induce the complex phases by incorporating the final-state interactions into the light-cone wavefunctions in the scalar and axial-vector diquark models, and then we calculate explicitly the Sivers and Boer-Mulders distribution functions from the light-cone wavefunction representations. The results are the same as those obtained from the direct calculation of the hadronic tensor without employing the concept of the light-cone wavefunction, since the essential interpretation of the final-state interaction is identical in both calculations. However, the analysis in this paper by using the light-cone wavefunction representations is useful for understanding the natures of the Sivers and Boer-Mulders distribution functions in a systematic way. In the light-cone wavefunction representations the Sivers distribution function is given by the overlap of the wavefunctions of the same quark spin states of the opposite nucleon spin states, whereas the Boer-Mulders distribution function is given by the overlap of the wavefunctions of the opposite quark spin states within a given nucleon spin state. From these properties of the light-cone wavefunction representations, we can understand why the Sivers distribution function has the opposite signs with the factor 3 difference in magnitude for the scalar and axial-vector diquark models, whereas the Boer-Mulders distribution function has the same sign and magnitude for these diquark models.

# Acknowledgments

This work was supported in part by the International Cooperation Program of the KICOS (Korea Foundation for International Cooperation of Science & Technology), and by the Korea Research Foundation Grant funded by the Korean Government (KRF-2008-313-C00166).

# References

- [1] S.J. Brodsky, D.S. Hwang, and I. Schmidt, Phys. Lett. B **530**, 99 (2002).
- [2] D.W. Sivers, Phys. Rev. D **41**, 83 (1990); Phys. Rev. D **43**, 261 (1991).
- [3] J.C. Collins, Phys. Lett. B **536**, 43 (2002).
- [4] X. Ji and F. Yuan, Phys. Lett. B **543**, 66 (2002).
- [5] A. Belitsky, X. Ji, and F. Yuan, Nucl. Phys. B **656**, 165 (2003).
- [6] D. Boer, S.J. Brodsky, and D.S. Hwang, Phys. Rev. D **67**, 054003 (2003).
- [7] D. Boer, P.J. Mulders, and F. Pijlman, Nucl. Phys. B **667**, 201 (2003).
- [8] D. Boer and P.J. Mulders, Phys. Rev. D **57**, 5780 (1998).
- [9] G.P. Lepage and S.J. Brodsky, Phys. Rev. D **22**, 2157 (1980).
- [10] S.J. Brodsky, H.C. Pauli, and S.S. Pinsky, Phys. Rep. **301**, 299 (1998).
- [11] S.J. Brodsky and S.D. Drell, Phys. Rev. D **22**, 2236 (1980).
- [12] S.J. Brodsky and D.S. Hwang, Nucl. Phys. B **543**, 239 (1999).
- [13] S.J. Brodsky, D.S. Hwang, B.-Q. Ma, and I. Schmidt, Nucl. Phys. B **593**, 311 (2001).
- [14] M. Diehl, T. Feldmann, R. Jakob, and P. Kroll, Nucl. Phys. B **596**, 33 (2001), Erratum-ibid. B **605**, 647 (2001).
- [15] S.J. Brodsky, M. Diehl, and D.S. Hwang, Nucl. Phys. B **596**, 99 (2001).
- [16] S.J. Brodsky, S. Gardner, and D.S. Hwang, Phys. Rev. D **73**, 036007 (2006).
- [17] S.J. Brodsky, D.S. Hwang, and I. Schmidt, Nucl. Phys. B **642**, 344 (2002).
- [18] D.S. Hwang, PoS (LC2008) 033; *Proceedings of LIGHT CONE 2008 Relativistic Nuclear and Particle Physics* (July 7-11, 2008, Mulhouse, France).
- [19] M. Burkardt and D.S. Hwang, Phys. Rev. D **69**, 074032 (2004).
- [20] R. Jakob, P.J. Mulders, and J. Rodrigues, Nucl. Phys. A **626**, 937 (1997).
- [21] J. Ellis, D.S. Hwang, and A. Kotzinian, Phys. Rev. D **80**, 074033 (2009).
- [22] M. Burkardt and B. Hannafious, Phys. Lett. B **658**, 130 (2008).